

Chapter III

Docking is the Rate-Limiting Step in a Bulk Fusion Assay

and Stimulated by V_C Peptide

3.1) Summary

In vitro vesicle fusion assays that monitor lipid mixing between t-SNARE and v-SNARE vesicles in bulk solution exhibit remarkably slow fusion on the non-physiological timescale of tens of minutes to several hours. Here single-vesicle, FRET-based assays cleanly separate docking and fusion steps for individual vesicle pairs containing full-length SNAREs. Docking is extremely inefficient and is the rate-limiting step. Importantly, the docking and fusion kinetics are comparable in both assays, one with v-SNARE vesicles tethered to a surface and the other with v-SNARE vesicles free in solution. Addition of the “V_C peptide” synaptobrevin-2 (57-92) increases the docking efficiency by a factor of ~30, but docking remains rate-limiting. In the presence of V_C peptide, the fusion step occurs on a timescale of ~10 s. In previous experiments using bulk fusion assays for which addition of synaptotagmin/Ca²⁺, Munc-18, or complexin accelerated the observed lipid-mixing rate, the enhancement might lie in the docking step, not the fusion step.

3.2) Introduction

Rothman and co-workers (Weber et al., 1998) were the first to show that v-SNARE-containing vesicles and t-SNARE-containing vesicles spontaneously fuse together in solution. Many labs have subsequently corroborated this result (James et al., 2008; Lu et al., 2006; Mahal et al., 2002; Martens et al., 2007; Pobbati et al., 2006; Rodkey et al., 2008; Schaub et al., 2006; Stein et al., 2007; Tucker et al., 2004; Xue et al., 2008). These experiments showed that formation of *trans*-vesicle SNARE complexes provides sufficient energy to overcome the intrinsic barrier to vesicle-vesicle fusion. However, the timescale of these bulk fusion reactions (minutes to hours) does not begin to mimic the timescale of Ca^2 -triggered neuronal exocytosis (high μs to ms) (Chapman, 2008). The overall fusion timescale is reduced by more than an order of magnitude on addition of a soluble peptide comprising residues 57-92 of syb in the vesicle mixture (Melia et al., 2002). This peptide is commonly referred to as “ V_C peptide” because it is a C-terminal fragment of the syb SNARE motif.

A major shortcoming of bulk SNARE-driven vesicle fusion assays thus far is the inability to separate in time the vesicle-vesicle *docking* step from the subsequent lipid mixing, or *fusion* step (Fig. 3-1). Either step could be rate-limiting and thus the underlying cause of the slow overall reaction rate. Using the new *single-vesicle docking and fusion assay* we cleanly separate the SNARE-mediated docking and fusion kinetics in this reconstituted system.

3.3) Results

First, we carried out a traditional bulk fusion assay (Weber et al., 1998), which monitors the progress of overall lipid mixing but does not dissect docking from fusion. Next, in order to evaluate the kinetics of the docking reaction (second-order rate constant k_{dock}) separately from the subsequent fusion reaction (first-order rate constant k_{fus}) (Fig. 3-1), we studied free t-SNARE vesicles docking and fusing with *individual* v-SNARE vesicles tethered to a passivated surface. Finally, to directly compare the tethered vesicle results to the traditional bulk experiment, we monitored the progress of docking and fusion in the bulk assay by periodically plating a sample of the vesicle mixture sparsely onto glass and directly counting instances of docking and fusion using the same single-vesicle FRET measurements as in the tethered vesicle assay.

Bulk Fusion Assay and Controls

Using a FRET-based bulk fusion assay we found that full-length neuronal SNARE proteins drive lipid mixing between unilamellar phospholipid vesicles of ~50 nm diameter at 37°C (Figs. 3-2 and 3-3), as reported previously by other laboratories (Chen et al., 2006; Gaffaney et al., 2008; Melia et al., 2002; Weber et al., 1998). In Fig. 3-2, lipid mixing is detected by exciting DiI (green fluorescent FRET donor labels present at 2% in the t-SNARE vesicle membranes) and measuring the red fluorescence intensity from FRET to DiD (FRET acceptor labels, present at 2% in the v-SNARE vesicle membranes). FRET occurs efficiently once v- and t-SNARE vesicles have undergone lipid mixing and both labels are present in the same membrane. When we mixed together t- and v-SNARE vesicles at 10 nM and 5 nM (in vesicles per liter), respectively, the amount of fluorescence intensity from FRET increases over the

course of the 120 min experiment (curve “-V_C” in Fig. 3-2 *a*). Replacing the DiD labels in the v-SNARE vesicles with NBD and Rhodamine and removing the DiI labels from the t-SNARE vesicles allowed us to test our vesicles using a standard dequenching assay in which the extent of lipid mixing is reported on a calibrated scale. The composite rate of docking and fusion of our vesicles is consistent with previous published results using similar materials and conditions (Fig. 3-3) (Chen et al., 2006; Gaffaney et al., 2008; Melia et al., 2002; Weber et al., 1998).

Addition of V_C peptide to the v- and t-SNARE vesicle mixture greatly enhanced the rate of lipid mixing (curve “+V_C” in Fig. 3-2 *a*). The optimized V_C peptide concentration of 4 μM (Fig. 3-2 *b*) (Chicka et al., 2008; Melia et al., 2002), caused a ~30-fold enhancement in the FRET signal after 35 min. We did not detect FRET for the following control mixtures (overlapping curves labeled “controls” in Fig. 3-2 *a*): (1) v-SNARE vesicles mixed with protein-free vesicles; (2) v-SNARE vesicles mixed with syx-only vesicles (lacking SNAP-25), and v-SNARE vesicles mixed with vesicles containing syx plus SNAP-25 missing its 26 most C-terminal amino-acid residues (t-SNAREs designed to mimic the BoNT/E cleavage product) (3) in the absence or (4) in the presence of 4 μM V_C peptide. Evidently all three SNARE proteins: syb, syx, and SNAP-25, are required for vesicle fusion on a 120-min timescale.

Docking and Fusion Assay Using Tethered v-SNARE Vesicles

To monitor docking and fusion between individual pairs of SNARE-bearing vesicles (Fig. 3-1), we tethered the v-SNARE vesicles to a polymer-containing lipid bilayer via biotin-NeutrAvidin interactions (Figs. 2-1 and 3-4) (Yoon et al., 2006). We incubated a sparse field of tethered v-SNARE vesicles with 10 nM t-SNARE vesicles in the presence or absence of 5 μM

V_C peptide. After reaction time intervals of 5-140 min, we rinsed the sample and imaged the surface at several locations to generate a single data set involving 1500-3000 tethered v-SNARE vesicles at each reaction time. Each reaction interval involved an entirely new surface. We took two images of the sample in rapid succession using a sensitive CCD camera, the first during laser excitation at 633 nm and the second at 514 nm (details in Methods) (Kapanidis et al., 2004; Wang et al., 2009). The first image located the tethered v-SNARE vesicles, while the second image located t-SNARE vesicles. From these images we directly counted instances of v- and t-SNARE co-localization and determined the FRET efficiency between co-localized pairs (Fig. 3-4).

Tethered Vesicle Docking and Fusion Rate Constants With and Without V_C Peptide

Histograms summarizing the absolute FRET efficiency E of *co-localized* vesicle pairs at three different reaction times are shown in Fig. 3-5, both in the absence (Fig. 3-5 *a*) and presence (Fig. 3-5 *b*) of V_C peptide. In each of the FRET efficiency histograms, there is a sharp peak centered at $E = 0$ and also a broad distribution of non-zero values centered at $E = 0.6-0.7$. The amplitude of the non-zero FRET peak grows as a function of reaction time. Histograms showing the distributions of the v-SNARE vesicle FRET intensities are shown in Fig. 3-6.

In order to interpret the FRET efficiency data, we used Förster theory and model configurations to calculate the range of FRET efficiencies that arise from three different conditions: a vesicle pair that is docked but unfused, docked and hemifused (outer leaflets mixed), or docked and fully fused (complete lipid mixing). The calculations (described in detail in Chapter II) take into account the size distributions of the v- and t-SNARE vesicles (Fig. 2-1)

and the Förster radius of the DiI-DiD FRET pair (Fig. 2-2). The modeling predicts a wide range of FRET efficiency values for each condition due to the distribution of vesicle sizes. However, for the vast majority of pairs, vesicles in a *docked but unfused* state will have $E \leq 0.25$ (Fig. 2-3), while vesicles that are *docked and fused* will have $E > 0.25$ (Fig. 2-4). Our calculations indicate that for any particular vesicle pair the FRET efficiency after full fusion is only 0.05-0.2 greater than the FRET efficiency after hemifusion. Depending on the size combination of a specific vesicle pair, the range of FRET efficiencies expected for hemifusion is $E = 0.15-0.9$, while the range of FRET efficiencies expected for full fusion is $E = 0.25-0.95$ (Fig. 2-4). Thus a population of hemifused vesicle pairs cannot be clearly distinguished from a population of fully fused vesicle pairs using the DiI/DiD FRET pair at 2 mol% labeling fraction.

The $E = 0.25$ FRET efficiency threshold suggested by the modeling is consistent with real-time observations of vesicle pairs as they dock and fuse (Fig. 3-7). Docked vesicle pairs make an abrupt transition from a low-FRET state ($E = 0-0.25$) to a stable high-FRET state ($E = 0.5-0.95$). The observed range of low FRET efficiencies is consistent with the model estimates for vesicle pairs in a docked but unfused state, and the observed range of high FRET efficiencies is consistent with the model estimates for the docked and fused (or hemifused) state. Accordingly, we use $E = 0.25$ as the value that separates v-SNARE/t-SNARE vesicle pairs that are docked but unfused from those that are docked and fused (Fig. 3-8). Again, “docked and fused” may include vesicle pairs that have undergone partial lipid mixing, including hemifusion. The docked but unfused curves are corrected statistically for the probability that a non-specifically bound t-SNARE vesicle happens to co-localize with a v-SNARE vesicle within our spatial resolution (“false co-localizations”). The corrected docking curves are determined both in the absence (Fig. 3-8 *a* and *b*) and the presence (Fig. 3-8 *c* and *d*) of V_C peptide. The “Total

“Docked” curves in Figs. 3-8 *b* and *d* are the sum of the “Docked and Fused” and the “Docked but Unfused” curves in Figs. 3-8 *a* and *c*.

The percentage of v-SNARE vesicles that are docked and fused grows to ~10% over 120 min without V_C peptide (Fig. 3-8 *a*) and to ~70% over 30 min with V_C peptide (Fig. 3-8 *c*). The latter curve plateaus at that level; some 30% of tethered v-SNARE vesicles never dock a t-SNARE vesicle on an 80-min timescale. Strikingly, in neither case do we clearly observe docked but unfused vesicle pairs within any of the 5 min measurement time intervals. The $E = 0$ peak of the FRET efficiency histograms (Fig. 3-5) arises almost entirely from false co-localization events, and its variability in amplitude reflects variability in the passivation of the surface. There are significantly fewer $E = 0$ events in the presence of V_C peptide. This is expected because the density of docked and fused pairs is much higher with V_C peptide. False-co-localization of a t-SNARE vesicle with a docked and fused pair (which includes 50% of the tethered v-SNARE vesicles by $t = 15$ min) will give rise not to $E = 0$ but to a lower apparent E for the docked and fused pair. *With or without V_C peptide, docking essentially always leads to fusion within the five-minute timescale of the measurement intervals.*

We used the known t-SNARE vesicle concentration to convert the initial slope of the total docking curves (Fig. 3-8 *b* and 3-8 *d*) into an approximate rate constant $k_{dock,teth}$ for docking between t-SNARE vesicles and tethered v-SNARE vesicles by assuming the reaction follows bimolecular kinetics. The linear fits are indicated by the dotted lines in Fig. 3-8 *b* and 3-8 *d*. In the absence of V_C peptide $k_{dock,teth} = (1.2 \pm 0.1) \times 10^3 \text{ M}^{-1} \cdot \text{s}^{-1}$, where the concentration is expressed as moles of vesicles per L. In the presence of V_C peptide, the same analysis gives $k_{dock,teth} = (4.2 \pm 0.3) \times 10^4 \text{ M}^{-1} \cdot \text{s}^{-1}$. V_C peptide enhances the docking efficiency in the tethered-vesicle assay by a factor of ~35.

Next, to estimate the fusion rate k_{fus} in the presence of V_C peptide, we directly observed individual docking and fusion events between free t-SNARE vesicles and tethered v-SNARE vesicles. Using 200 ms exposures and 3 s cycle time, we observed individual t-SNARE vesicles dock (co-localize) and fuse with individual tethered v-SNARE vesicles. Fusion was observed as the sudden appearance of red fluorescence from FRET simultaneous with a loss of co-localized green intensity. See Fig. 3-14 for a sample fusion event. The observed fusion was sensitive to the presence of intact SNAP-25. Incubation of tethered v-SNARE vesicles with vesicles whose t-SNAREs mimic the BoNT/E cleavage product in the presence of V_C peptide resulted in no observable fusion over 15 min of observation time.

We observed dozens of individual docking and fusion events. A histogram of τ_{fus} values (Fig. 3-9) was generated for 36 fusion events for which the docking time could be clearly discerned. For 85% of the fusion events the delay time between docking and fusion lies in the range <3 s to 42 s. More than half of the fusion events occurred < 10 s after docking, while a few events occurred on a 2-5-min timescale. The fusion kinetics are inhomogeneous, but evidently the majority of the sample has $k_{fus} \sim 0.1 \text{ s}^{-1}$. In the absence of V_C peptide, the very slow rate of docking precluded observation of individual fusion events.

Single-vesicle FRET Analysis of Bulk Vesicle Mixtures

Finally, to directly compare results from the bulk assay and the tethered vesicle assay, we mixed together v- and t-SNARE vesicles in the usual bulk conditions (as in Fig. 3-2). At varying reaction times over the course of 2-3 h, we removed a small sample from the mixture, quickly diluted it by a factor of 1000, and then plated the vesicles and vesicle pairs sparsely onto a glass

coverslip for two-color imaging with alternating laser excitation. The time lag between dilution of the sample and imaging was <10 min for each data point. At each reaction time point, some 100-500 individual v-SNARE vesicles contributed to the data set. Histograms showing the FRET efficiencies E of co-localized v- and t-SNARE vesicle pairs are shown in the absence (Fig. 3-10 *a*) and presence (Fig. 3-10 *b*) of V_C peptide. Histograms of all of v-SNARE vesicle FRET intensities are found in Fig. 3-11 *a* and *b*. The main feature of each FRET efficiency histogram is a broad distribution of non-zero values centered at $E = 0.6-0.7$, which grows in as a function of reaction time. There is little or no $E = 0$ peak in Fig. 3-10 because the sparse plating of the bulk mixture essentially eliminates false co-localization of undocked vesicle pairs.

We distinguished docked but unfused from docked and fused (or hemifused) pairs using the same $E = 0.25$ FRET efficiency threshold. After correcting for $E = 0$ events that arise from false co-localizations between vesicles, docking curves were determined for v- and t-SNARE vesicles both in the absence (Fig. 3-12 *a* and *b*) and in the presence (Fig. 3-12 *c* and *d*) of V_C peptide. The bulk assay docking curves (Fig. 3-12) are qualitatively similar to those from the tethered-vesicle assay (Fig. 3-8). Again, we found no statistically significant evidence of *any* docked but unfused vesicle pairs, indicating that docking is also the slow step in the bulk vesicle fusion assay. The initial slope of the docking curve without V_C peptide (Fig. 3-12 *b*) gives the estimate $k_{dock,bulk} = (4.7 \pm 0.2) \times 10^3 \text{ M}^{-1} \cdot \text{s}^{-1}$. In the presence of V_C peptide (Fig. 3-12 *d*), $k_{dock,bulk} = (11 \pm 2) \times 10^4 \text{ M}^{-1} \cdot \text{s}^{-1}$. Both with and without V_C peptide, the k_{dock} values in bulk are three to four times those from the tethered-vesicle assay, suggesting that tethering hinders the docking efficiency.

As a control, we incubated v-SNARE vesicles with DiI-labeled protein-free vesicles in bulk for three hours and then plated a diluted sample onto glass. This yielded no significant

FRET between labels (Fig. 3-11 *c* and *d*). We also incubated v-SNARE vesicles with V_C peptide plus DiI-labeled t-SNARE vesicles that mimic the t-SNAREs following BoNT/E cleavage (Fig. 3-11 *e*) and again found no significant FRET. Evidently there is no significant exchange of donor/acceptor labels between vesicles on a 3-h timescale, nor does immobilization onto a glass surface induce substantial lipid mixing. These controls suggest that our method may prove useful in the analysis of docking and fusion kinetics in bulk fusion assays in the future.

3.4) Discussion

Experimental Docking Rate

In 1998, Rothman and co-workers were the first to show that full-length neuronal SNARE proteins are capable of catalyzing vesicle-vesicle fusion in vitro (Weber et al., 1998). In the intervening 12 years, we estimate that 33 papers have described neuronal SNARE-induced bulk vesicle fusion. The papers report the effects of SNARE truncations (McNew et al., 1999; Parlati et al., 1999); of adding presynaptic proteins such as synaptotagmins (Bhalla et al., 2008; Chicka et al., 2008; Gaffaney et al., 2008; Hui et al., 2009; Mahal et al., 2002; Martens et al., 2007; Stein et al., 2007; Tucker et al., 2004; Xue et al., 2008), double C2 domain (doc2) proteins (Groffen et al.), Munc-18 (Rodkey et al., 2008; Shen et al., 2007), the Ca^{2+} -dependent activator protein for secretion (CAPS)

(James et al., 2008; James et al., 2009), complexins (Chicka and Chapman, 2009; Malsam et al., 2009; Schaub et al., 2006; Seiler et al., 2009), calmodulin (Siddiqui et al., 2007), and synaptophysin (Siddiqui et al., 2007); of adding synthetic PEG polymers (Dennison et al., 2006) and peptides (Chicka et al., 2008; Melia et al., 2002; Pobbaty et al., 2006); and of changing the lipid content (Melia et al., 2006), reconstitution method (Chen et al., 2006), or protein to lipid ratio (Lu et al., 2005). One result in common is the extremely slow *composite* timescale of docking and fusion (tens of min to a few hr) relative to the timescale of fusion in vivo (hundreds of μs to a few ms) (Chapman, 2008).

Here we have repeated the bulk fusion assay using vesicles reconstituted with a syb concentration that approximates the surface density in synaptic vesicles (Takamori et al., 2006).

The v-SNARE vesicles dock and fuse with t-SNARE vesicles in bulk solution on a 1-2 hr timescale (Fig. S2), in qualitative agreement with bulk fusion experiments performed under similar conditions in other labs (Chen et al., 2006; Gaffaney et al., 2008; Melia et al., 2002; Weber et al., 1998). To dissect the vesicle-vesicle docking kinetics, we sampled the bulk fusion mixture at ~15 min intervals over a 120 min period, plated the vesicles sparsely onto glass, and directly interrogated them using alternating laser excitation two-color fluorescence microscopy (Schuette et al., 2004). This enabled us to directly count instances of co-localization between single t- and v-SNARE vesicles, yielding an effective bimolecular docking rate constant

$$k_{dock,bulk} = (4.7 \pm 0.2) \times 10^3 \text{ M}^{-1} \cdot \text{s}^{-1}.$$

At concentrations of 5 nM v-SNARE vesicles and 10 nM t-SNARE vesicles, the time at which half the v-SNARE vesicles have undergone at least one docking event to a t-SNARE vesicle is ~ 200 min. Quantitative measurement of single vesicle pairs' FRET efficiency and interpretation of the FRET efficiency values using Förster theory and model configurations showed that 589 of 606 (97%) of docked v- and t-SNARE vesicle pairs had fused together prior to the 10-min timescale of the measurement. Addition of V_C peptide, syb(57-92), to the SNARE-bearing vesicle mixture resulted in $k_{dock,bulk} = (11 \pm 2) \times 10^4 \text{ M}^{-1} \cdot \text{s}^{-1}$, a ~25-fold enhancement of the docking rate constant. A similar 2336 of 2398 docked pairs (97%) had fused before the measurement. Our modeling showed that using DiI/DiD FRET pair at 2% labeling fraction we cannot distinguish between populations of hemifused and fully fused vesicle pairs. Therefore our “docked and fused” population may include vesicles that are hemifused/partially mixed. This argues against a previous assignment of $E = 0.35$ to the hemifusion state (Yoon et al., 2008; Yoon et al., 2006).

For comparison, we also studied free t-SNARE vesicles docking and fusing with v-SNARE vesicles that had been tethered to a passivated PEG surface. The resulting docking rate constants were $k_{dock,teth} = (1.2 \pm 0.1) \times 10^3 \text{ M}^{-1}\cdot\text{s}^{-1}$ in the absence of V_C peptide and $k_{dock,teth} = (4.2 \pm 0.3) \times 10^4 \text{ M}^{-1}\cdot\text{s}^{-1}$ in the presence of V_C peptide. Again, we again did not observe any appreciable accumulation of docked but unfused intermediates; we estimate that 648 of 672 (96%) of docked pairs without V_C peptide and 8364 of 8799 (95%) of docked pairs with V_C peptide had fused within the 5 min time resolution of the measurement. In combination, the results indicate that in the bulk sampling experiments the glass surface did not induce the observed fusion to an appreciable extent. *The near absence of docked but unfused v-SNARE/t-SNARE vesicle pairs in both experiments clearly demonstrates that docking is the rate-limiting step in the vesicle-vesicle fusion reaction.*

Finally, by directly monitoring single docking and fusion events in the tethered-vesicle assay in the presence of V_C peptide in real time, we showed that the majority of docked vesicles fuse in ~10 s. For comparison, the characteristic timescale on which a single tethered v-SNARE vesicle docks its first t-SNARE vesicle in the presence of V_C peptide at concentration of 10 nM is $\tau_{dock} = (10 \text{ nM} \times 4.2 \times 10^4 \text{ M}^{-1}\cdot\text{s}^{-1})^{-1} = 2400 \text{ s} = 40 \text{ min}$, ~200 times longer than the fusion timescale. Direct observation of $k_{fus} \sim 0.1 \text{ s}^{-1}$ further demonstrates that docking is the slow step in the presence of V_C peptide. We were unable to study individual docking and fusion events in the absence of V_C because the docking efficiency was too low.

Simple Docking Model

Here we compare the experimental docking rate constants with a simple estimate of the rate k_{V+T} of vesicle-vesicle “close encounters” in order to estimate the docking efficiency per

encounter. The diffusion-limited rate constant for collisions between two freely diffusing spheres in bulk solution is given by (Berg, 1993):

$$k_{\text{diff}} = 4\pi N_A (R_V + R_T)(D_V + D_T) \quad (13)$$

The rate constant has units of $\text{M}^{-1}\cdot\text{s}^{-1}$; here the molarity is defined as moles of vesicles per L, N_A is Avogadro's number, R_V and R_T are the v- and t-SNARE vesicle radii, and D_V and D_T are their diffusion coefficients. For our vesicles $R_V \sim R_T \sim 25 \text{ nm}$ and $D_V \sim D_T \sim 3.3 \times 10^{-8} \text{ cm}^2\cdot\text{s}^{-1}$ (Schuette et al., 2004), yielding $k_{\text{diff}} \sim 2.5 \times 10^9 \text{ M}^{-1}\cdot\text{s}^{-1}$.

However, the incomplete surface coverage of v- and t-SNARE protein causes k_{V+T} to be smaller than k_{diff} . We define k_{V+T} as the rate constant for complementary t-SNARE and v-SNARE proteins on two different vesicles to come into close enough proximity to "touch" and potentially form a SNARE complex. To better estimate this "close encounter" rate, we use a simple model which treats t-SNAREs and v-SNAREs as immobile, disk-shaped absorbing patches with common radius $s_i = 2 \text{ nm}$ (Fig. 3-13). As shown by Berg (Berg, 1993), a fairly sparse set of such absorbing disks on the surface of a sphere can cause diffusive flux onto the sphere comparable to the case in which the entire sphere is absorbing (as in Eq. 13 above). In comparison with a completely absorbing sphere, the diffusive flux for a sphere partially covered by absorbing patches is diminished by a correction factor of $(1 + \pi R_i/N_i s_i)^{-1}$, where R_i is the target vesicle radius, N_i is the number of absorbing disks, s_i is the radius of each disk, and $i = T$ or V labels the type of vesicle. This factor approaches 1 as $N_i s_i$ becomes large; it approaches 0 as $N_i s_i$ approaches 0; and it is $\frac{1}{2}$ when $N_i s_i = \pi R_i$.

Our refined formula for the rate constant for vesicle-vesicle encounters in which a t-SNARE "touches" a v-SNARE in bulk solution becomes:

$$k_{V+T} = k_{diff}(1 + \pi R_T / N_T s_T)^{-1} (1 + \pi R_V / N_V s_V)^{-1} \quad (14)$$

In our case, using $N_T = 65$ t-SNAREs per vesicle, $N_V = 45$ v-SNAREs per vesicle, and using the rough estimate $s_T = s_V = 2$ nm the correction factor becomes ~ 0.6 for t-SNARE vesicles and ~ 0.5 for the v-SNARE vesicles. The overall close encounter rate constant is

$k_{V+T} \sim 0.3$ $k_{diff} \sim 8 \times 10^8$ M⁻¹·s⁻¹. The estimated probability of successful docking per effective encounter event (p_{dock}) is then the ratio of our experimentally-derived docking rate constant k_{dock} to k_{V+T} .

In the bulk fusion assay, this yields $p_{dock} = k_{dock,bulk} / k_{V+T} \sim 6 \times 10^{-6}$ without V_C peptide and $p_{dock} \sim 1.4 \times 10^{-4}$ with V_C peptide. In the absence of V_C peptide, roughly 170,000 close encounters are required to form one docked vesicle pair; with V_C peptide, roughly 7000 close encounters are required. Such low values of p_{dock} strongly suggest that typical v-SNARE/t-SNARE pairs are *highly inert*, i.e., unable to form *trans*-vesicle SNARE complexes on the timescale of the collision. The estimated values of p_{dock} for the tethered-vesicle assay would be even smaller, perhaps due to geometric constraints on the approach of t-SNARE vesicles to tethered v-SNARE vesicles or to some degree of interference by the nearby passivated surface.

Mechanistic Implications

By using the same materials in bulk and single-vesicle assays, our experiments clearly show that docking is the rate-limiting step in a bulk vesicle-vesicle fusion reaction driven by full-length neuronal SNARE proteins. *In our assay, enhancement of the overall fusion kinetics by addition of V_C peptide is entirely due to enhancement of the docking efficiency, not to any direct effect on the fusion step.* A clean comparison with experiments performed in other laboratories is

frustrated by wide variability in the proteins, lipid compositions, protein to lipid ratios, detergents, protein and vesicle purification procedures, vesicle concentrations, and temperatures used to study this reaction. Nevertheless, our results may have widespread significance for proper interpretation of other bulk fusion assays.

Previous studies have reported enhancement of the lipid mixing rate between vesicles containing full-length neuronal SNAREs in the presence of: (1) synaptotagmin1 (syt1) (Loewen et al., 2006; Mahal et al., 2002); (2) the soluble domain of syt1, C2AB, either in the absence (Mahal et al., 2002) or presence of Ca^{2+} (Bhalla et al., 2008; Bhalla et al., 2005; Chicka and Chapman, 2009; Chicka et al., 2008; Gaffaney et al., 2008; Hui et al., 2009; Martens et al., 2007; Schaub et al., 2006; Tucker et al., 2004); (3) the soluble domains of other synaptotagmin isoforms (Bhalla et al., 2008; Bhalla et al., 2005); (4) CAPS, the Ca^{2+} -dependent activator protein for secretion (James et al., 2008; James et al., 2009); and (5) doc2 proteins (Groffen et al.). *All of these results may arise from increased docking efficiency in the presence of the accessory protein, not acceleration of the transition from the docked state to the fused state.* Our data is also consistent with the suggestion that low temperature pre-incubations that give rise to a burst of fast lipid mixing (Malsam et al., 2009; Parlati et al., 1999; Rodkey et al., 2008; Seiler et al., 2009; Shen et al., 2007; Weber et al., 1998) accumulate docked but unfused vesicle pairs that fuse simultaneously once the temperature is raised to 37°C.

In our bulk assay, addition of V_C peptide enhances $k_{dock,bulk}$ by more than an order of magnitude. Presumably V_C peptide binds to the C-terminus of the SNARE motif of syx and SNAP-25, where the corresponding amino acids in syb bind in the ternary SNARE complex (Melia et al., 2002; Sutton et al., 1998). Work with soluble protein domains suggested that V_C peptide may help prevent formation of off-pathway 2:1 syx:SNAP-25 complexes (Pobatti et al.,

2006). However, our t-SNAREs are co-expressed in bacteria and are present in a 1:1 overall syx:SNAP-25 stoichiometry in the vesicle, indicating that 2:1 complexes are not important here. In other studies, V_C peptide stimulated bulk vesicle-vesicle lipid mixing to a similar extent whether or not the “H_{abc}” domain was present (Melia et al., 2002), which argues against a large effect due to V_C stabilization of the “open” syx conformation. In addition, previous work showed that reconstitution of t-SNARE vesicles with a constitutively “open” syx mutant does not affect bulk vesicle-vesicle lipid mixing kinetics (Shen et al., 2007).

Considering all of these results, we suggest that the V_C peptide may stimulate docking by nucleating t-SNARE folding upon binding. Accordingly, CD spectroscopy on the soluble SNARE domains (Pobbatte et al., 2006) and proteolysis protection experiments on full-length SNAREs reconstituted into vesicles (Melia et al., 2002) suggest that the t-SNAREs assume a more ordered secondary structure in the presence of V_C peptide. However, we cannot exclude the possibility that the presence of V_C peptide simply helps prevent the t-SNAREs from self-aggregating into large, inert “mounds,” as directly observed in AFM studies of supported lipid bilayers made from t-SNARE vesicles (Liu et al., 2005).

The neuronal proteins syt1 (Chicka and Chapman, 2009; Chicka et al., 2008; Gaffaney et al., 2008; Hui et al., 2009; Loewen et al., 2006; Lu et al., 2006; Mahal et al., 2002; Martens et al., 2007; Schaub et al., 2006; Stein et al., 2007; Tucker et al., 2004; Xue et al., 2008), CAPS (James et al., 2008; James et al., 2009), and doc2 (Groffen et al.), have all been shown to bind t-SNAREs in vitro. It seems entirely possible that these proteins may enhance docking by a similar mechanism as V_C peptide, either by nucleating folding within the 1:1 t-SNARE acceptor complex (Weninger et al., 2008) or by reducing t-SNARE self-aggregation.

Comparison with other docking and fusion assays

While we have shown that for our materials docking is the slow step in both the bulk and single-vesicle assays, there remains tremendous variability among the results of single- or few-vesicle assays capable of separating the docking kinetics from the fusion kinetics. In a similar tethered vesicle assay using neuronal SNAREs, Shin and co-workers (Yoon et al., 2008) found that 27% of tethered v-SNARE vesicles docked a t-SNARE vesicle from solution after 15 min when the t-SNARE vesicles were present at only 200 pM in the absence of V_C peptide. This is much more efficient docking than in our assay. However, the docked vesicle pairs fused together on a timescale of tens of minutes, much less rapidly than ours (Yoon et al., 2008). The most obvious difference between their experiment and ours is the use of an N-terminally truncated version of syx (residues 168-288), which lacks the H_{abc} domain. In addition, their t-SNARE vesicles were made by expressing and purifying syx and SNAP-25 separately, mixing the proteins together in detergent, and then mixing the protein/detergent solution with pre-formed vesicles. The method of reconstitution may well be an important variable.

Walla and co-workers (Cypionka et al., 2009) used fluorescence cross-correlation spectroscopy (FCCS) and fluorescence lifetime measurements to monitor docking and fusion between v- and t-SNARE vesicles in solution at room temperature. Their t-SNARE vesicles contained a “stabilized acceptor complex,” which included syx(183-288), SNAP-25, and syb(49-96), a peptide similar to the V_C peptide (syb(57-92)). The vesicles also contained 10% cholesterol and phospholipids derived from bovine brain. At vesicle concentrations of 1-10 nM each, they observed quite efficient docking with a time constant of 70 s, followed by fusion with

a time constant of 840 s. These results are again very different from ours. The FCCS study again used truncated syx rather than the full-length syx used here.

Several other groups have developed in vitro assays that resolve docking from fusion by monitoring single v-SNARE vesicles interacting with a supported lipid bilayer containing t-SNARE proteins (Bowen et al., 2004; Domanska et al., 2009; Fix et al., 2004; Karatekin et al.; Liu et al., 2005). The docking and fusion kinetics derived from these experiments vary tremendously and cannot be directly compared with bulk fusion experiments.

3.5) Experimental Procedures

Peptide Synthesis

A peptide derived from the C-terminus of syb (aa 57- 92, the V_C peptide) was synthesized by the University of Wisconsin-Madison Biotechnology Center. The peptide was purified with high-pressure liquid chromatography to ~80% purity.

Bulk Fusion Experiments

We carried out bulk vesicle fusion experiments presented in Fig. 3-2 *a,b* in 96-well FluoroNunc plates (Nunc/**Thermo Fisher Scientific**, Rochester, NY). Each well of the microplate contained 125 µL total volume, including 5 nM DiD-labeled v-SNARE vesicles and 10 nM DiI-labeled t-SNARE vesicles in Fusion Buffer (25 mM HEPES-KOH, 100 mM KCl, 0.2 mM EGTA, and 1 mM dithiothreitol, pH 7.40). Lipid mixing was observed as an increase in FRET from DiI labels, which were reconstituted into t-SNARE vesicle membranes, to DiD labels, which were reconstituted into v-SNARE vesicle membranes, by measuring DiD (acceptor) fluorescence at 700 ± 4.5 nm during DiI (donor) excitation at 514 ± 4.5 nm using a microplate reader (Molecular Devices SpectraMAX Gemini, Sunnyvale, CA). For the control experiments shown in Fig. S1*a*, the exact volume of DiI-labeled control vesicles (protein free, BoNT/E cleavage simulation, syx only) was adjusted such that each sample had a constant absorbance at 514 nm (Varian Cary 50 UV/Vis Spectrophotometer, Palo Alto, CA). The vesicles were pre-warmed to 37°C prior to mixing.

The bulk vesicle-vesicle fusion experiment shown in Fig. 3-3 used vesicles prepared identically to the DiD- and DiI-labeled vesicles. The only difference was that the v-SNARE vesicles were reconstituted to include 1.5% N-(7-nitro-2-1,3-benzoxadiazol-4-yl)-1,2-dipalmitoyl phosphatidylethanolamine (NBD-PE) and 1.5% N-(lissamine rhodamine B sulfonyl)-1,2-dipalmitoyl phosphatidylethanolamine (Rhodamine-PE) and the t-SNARE vesicles were unlabeled. Lipid mixing was monitored by measuring NBD fluorescence at 530 ± 10 nm during excitation at 460 ± 20 nm using a microplate reader (BioTek Synergy HT, Winooski, VT). The vesicles were pre-warmed separately to 37°C prior to mixing at a 1:9 v-SNARE vesicle: t-SNARE vesicle ratio in a 96-well FluoroNunc plate (Nunc/**Thermo Fisher Scientific**, Rochester, NY). The total volume was $75 \mu\text{L}$, including 6.7 nM v-SNARE vesicles and 60 nM t-SNARE vesicles in Fusion Buffer. Fusion between the doubly-labeled v-SNARE vesicles and unlabeled t-SNARE vesicles caused the average distance between NBD and Rhodamine labels to increase, which decreased the efficiency of NBD FRET to Rhodamine and therefore increased NBD's fluorescence quantum yield. After three hours of incubation time $20 \mu\text{L}$ of *n*-dodecyl- β -D-maltoside was injected into the solution to a final concentration of 0.5% w/v. NBD fluorescence is plotted as a function of time in Fig. 3-3 by subtracting the initial fluorescence intensity value and then normalizing the fluorescence signal to the maximum NBD fluorescence measured after detergent addition. Lipid mixing between 6.7 nM v-SNARE vesicles and 60 nM t-SNARE vesicles was also assayed in the presence of 10 μM of the cytoplasmic domain of syb (aa 1-94).

Total Internal Reflection Fluorescence Microscopy

A modified commercial wide-field microscope (Eclipse TE2000-U, Nikon, Melville, NY) enabled selective excitation of fluorophores within ~200 nm of the glass/water interface using "through-the-objective" total internal reflection (TIR) (Axelrod, 2001). A 60 \times , 1.45 NA, oil-immersion objective (Olympus, Melville, NY) combined with the Nikon tube lens made the effective magnification of the microscope 90 \times .

Total internal reflection of lasers at 633 nm (HeNe, Coherent, Santa Clara, CA) and 514 nm (Ar⁺, Melles Griot, Carlsbad, CA) excited DiD and DiI, respectively. The evanescent wave generated by the 514 nm laser was >93% s-polarized. The two laser beams were combined using a 45° green reflective dichroic filter, (J47-268, Edmund Optics, Barrington, NJ) and then expanded together using a pair of achromatic lenses (Edmunds Optics, Barrington, NJ). Clipping the expanded laser beams using a rectangular slit prior to focusing onto the back focal plane of the objective created a rectangular region of excitation covering half of the field of view of the CCD camera. A dual band dichroic mirror 514/633PC (Chroma, Rockingham, VT) reflected the co-aligned laser beams and passed the fluorescence emission from both dyes. At the sample, the excitation intensity profile was flat to within 20% of the maximum value; the ratio of 633 nm to 514 nm intensity was constant to within 5% over the entire field of view.

Fluorescence was collected by the microscope objective, focused by the tube lens, and then collimated with an achromatic lens within a home-built dual-imaging chamber (Wang et al., 2009). A dichroic mirror reflecting 565-615 nm and passing longer wavelengths (Chroma) separated the fluorescence into “green” and “red” channels that passed emission filters HQ590/50M and HQ700/75M (Chroma), respectively. A positive lens with a long focal length was placed in the red channel such that both channels focused at the same plane. An identical dichroic mirror recombined the two channels and an achromatic lens focused them side-by-side

onto an electron-multiplying charge-coupled device camera (EMCCD, Model DV897-UVB, Andor Technologies, Belfast, Northern Ireland). The camera had $16 \times 16 \mu\text{m}^2$ pixels, which corresponded to $178 \times 178 \text{ nm}^2$ at the sample. Data acquisition was controlled through Andor Solis software (Andor Technologies). The mapping between the red and green channels was determined on a daily basis by imaging immobilized t-SNARE vesicles, which fluoresce in both channels at high laser power. The mapping function includes translation, rotation, and scaling; it maps a position in the red channel to the corresponding position in the green channel with an average deviation of 1.0 ± 0.5 pixels from the observed peak positions.

Single-Vesicle FRET Measurements

FRET efficiencies for isolated pairs of vesicles were determined from two dual-color, 50 ms camera exposures obtained in rapid succession using alternating laser excitation (ALEX) (Kapanidis et al., 2004). The first exposure used 1.4 W/cm^2 of 633 nm excitation and the second used 1.4 W/cm^2 of 514 nm excitation. The alternation period for the lasers was 100 ms and the duty cycle was 45-48%. The timing of the lasers was controlled using mechanical shutters (Model LS2Z2, Uniblitz, Rochester, NY), which opened with a time constant of < 1 ms in response to a pulse from the camera. While imaging tethered vesicles using ALEX, the frame rate is fast enough to essentially freeze vesicle motion during both measurements. The root-mean-square displacement of a tethered vesicle is estimated as $\sqrt{4D_{ves}\tau} = 0.1 \mu\text{m}$, where $D_{ves} \sim 0.05 \mu\text{m}^2 \cdot \text{s}^{-1}$ and $\tau = 50 \text{ ms}$ is the average time between frames. In other words, the average vesicle moves ~ 0.5 pixels between measurements.

The 633 nm laser exclusively excited the acceptor labels, permitting unambiguous localization of each v-SNARE vesicle. The fluorescence intensity of each individual v-SNARE vesicle, I_{red}^{633} , was determined after background-subtraction by integrating the total intensity present in a 7×7 pixel region centered at the highest-value pixel. The 514 nm laser strongly excited the donor labels in the t-SNARE vesicles, but also weakly excited the acceptor labels in the v-SNARE vesicles. The fluorescence intensity in the red and green channels during 514 nm excitation, I_{red}^{514} and I_{green}^{514} , respectively, was measured for each v-SNARE vesicle using the same region of integration as for measurement of I_{red}^{633} . The fluorescence intensity due to FRET, I_{FRET}^{514} , was determined from the measurement of I_{red}^{514} after subtracting contributions from the two major sources of cross-talk: leakage of donor (DiI) fluorescence into the red channel and direct excitation of the acceptor label (DiD) during 514 nm excitation:

$$I_{FRET}^{514} = I_{red}^{514} - \alpha I_{green}^{514} - \beta I_{red}^{633} \quad (15)$$

where α and β are the cross-talk correction factors. The correction factors were determined by measuring intensities for donor-only and acceptor-only vesicles and correcting to zero FRET intensity. For our system, $\alpha = 0.16$ and β was determined daily to account for differences in laser alignment and intensities.

FRET efficiencies are calculated for the subset of v-SNARE vesicles that were co-localized with a donor vesicle using the equation:

$$E = \frac{I_{FRET}^{514}}{I_{FRET}^{514} + \gamma I_{green}^{514}} \quad (16)$$

Here γ is a detection sensitivity factor that places DiI fluorescence collected in the green channel on the same scale as DiD fluorescence collected in the red channel. Co-localization includes both cases for which a donor vesicle emits green fluorescence in the same position as a v-SNARE vesicle and cases for which there is a significant amount of intensity from FRET. The second criterion finds vesicle pairs for which green fluorescence is not detected because of highly efficient FRET.

Vesicles containing both 1% DiD + 1% DiI were used to determine γ because these vesicles contain equal amounts of donor and acceptor labels and undergo almost complete FRET ($E = 0.9$). We first measured I_{FRET}^{514} for vesicles with high FRET, and then selectively bleached the acceptor labels using 633 nm. We then measured I_{green}^{514} using the same 514 nm laser power and image acquisition settings as for I_{FRET}^{514} . For both measurements DiI was excited at the same rate and fluorescence was collected for the same amount of time, so the ratio of the two intensities gave us γ , the relative detection efficiency for DiD fluorescence in the red channel versus DiI fluorescence in the green channel. Averaging over hundreds of vesicles gave us $\gamma = 2.0 \pm 0.1$.

The vesicles containing both 1% DiD + 1% DiI were also used to determine the relative excitation efficiencies of DiD at 633 nm versus DiI excitation at 514 nm. We imaged the mixed vesicles using 633 nm and 514 nm sequentially using the same image acquisition settings for both exposures. The total fluorescence collected was determined after correcting for differences in the collection efficiency (I_{red}^{633} vs $I_{FRET}^{514} + \gamma I_{green}^{514}$) for each individual mixed vesicle. The ratio of total collected fluorescence reflected the differences in excitation efficiency of DiD with 633 nm and of DiI at 514 nm at the relative laser powers used.

Statistical Correction for False Co-localizations

Non-specific binding of t-SNARE vesicles to the imperfectly passivated surface leads to “false co-localization” events in which a t-SNARE vesicle appears to be bound to a v-SNARE vesicle but in fact is not. Uncertainty in the location of a moving vesicle and in the mapping between the red and green channels cause us to classify t-SNARE vesicles (imaged in the green channel with 514 nm excitation) located within a 7×7 pixel ($1.25 \mu\text{m} \times 1.25 \mu\text{m}$) area surrounding a tethered vesicle (imaged in the red channel during 633 nm excitation) as co-localized. Such events include both false co-localizations and real events in which vesicle pairs have docked together. We estimate the number of low FRET (defined as $E < 0.25$) “false co-localizations” on each surface using the following statistical correction. First we assumed that non-specific binding of t-SNARE vesicles occurs with equal probability everywhere on the surface, i.e., that the number of non-specific binding events per surface area is constant. We measured the non-specific binding density (t-SNARE vesicles per μm^2) by analyzing regions of the surface lacking any v-SNARE vesicles. Any t-SNARE binding in these regions is due to non-specific interactions between the t-SNARE vesicle and the surface. For each image, we calculated the total area susceptible to low FRET false co-localizations from the total surface area co-localized with tethered vesicles after excluding high-FRET vesicle pairs. The product of the non-specific binding density and the area susceptible to low-FRET false co-localizations yields the number of low-FRET false co-localization events in an image. To determine the number of true docked but unfused events, this estimated low-FRET false co-localization count was subtracted from the total number of low-FRET co-localization events. High-FRET co-localization events in which a v-SNARE vesicle has docked and fused with a t-SNARE vesicle *and also* experiences false co-localization with another t-SNARE vesicle presumably

occur as well. For these events, the falsely co-localized green intensity will lower the apparent FRET efficiency of the docked and fused vesicle pair.

All data analysis was performed from raw images using custom computer programs written in MATLAB (The MathWorks, Natick, MA), which are freely available upon request. The programs use published peak finding strategies
<http://www.physics.georgetown.edu/matlab/index.html> (Crocker and Grier, 1996).

3.6) Figures

Figure 3-1

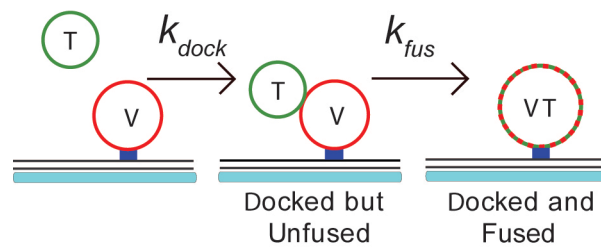
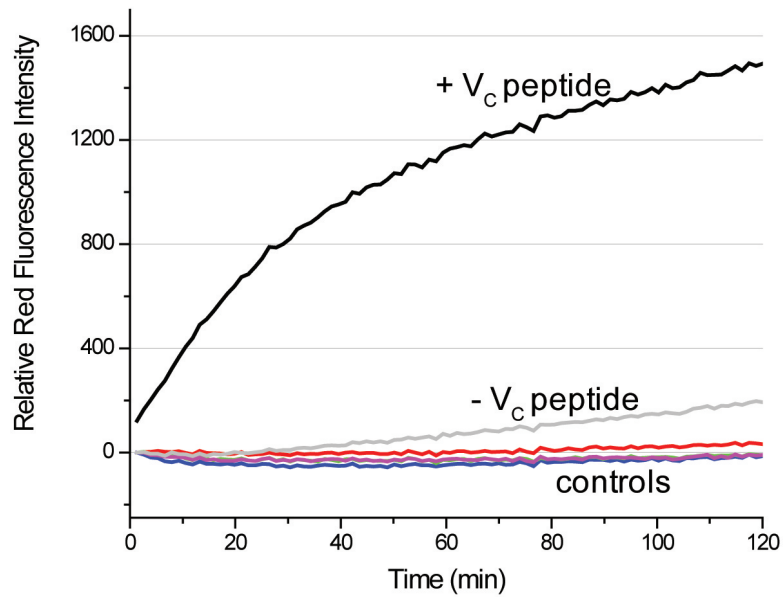


Figure 3-1. Two Step Model of SNARE-Driven Vesicle-Vesicle Docking and Fusion

The t-SNARE vesicles (T) dock (second-order rate constant k_{dock}) and fuse (first-order rate constant k_{fus}) with v-SNARE vesicles (V). The single-vesicle assay resolves these two steps. Docked but unfused pairs of vesicles differ from docked and fused pairs in the measured FRET efficiency from green labels in the t-SNARE vesicles to red labels in the v-SNARE vesicles.

Figure 3-2

a.



b.

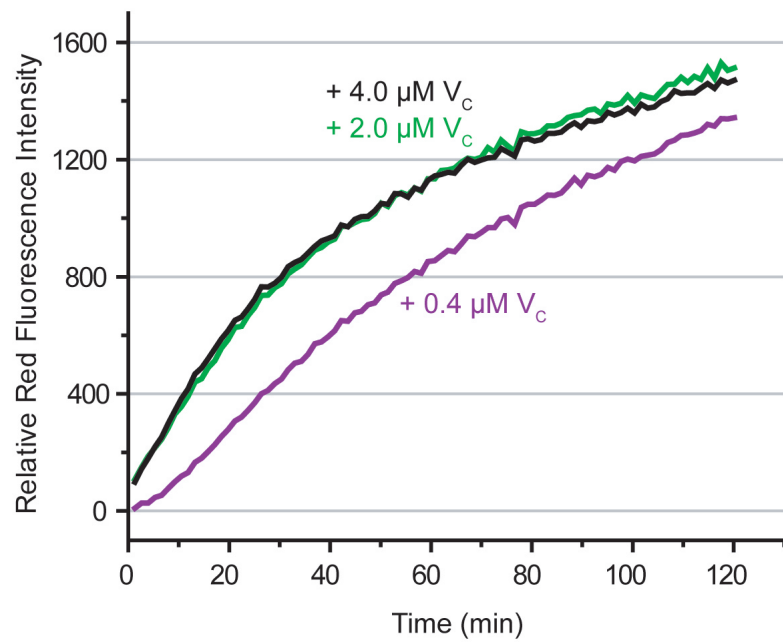


Figure 3-2. Bulk Lipid Mixing from FRET Assay With and Without V_C Peptide

Composite rate of vesicle-vesicle docking and fusion determined using bulk fusion assay. *a)* Red fluorescence measured during green excitation from a bulk mixture of 5 nM v-SNARE vesicles labeled with 2% DiD and 10 nM t-SNARE vesicles labeled with 2% DiI in the presence (+ V_C) and absence (−V_C) of 4 μM V_C peptide. Controls: No significant lipid mixing occurs if v-SNARE vesicles are mixed with vesicles that have one or both t-SNARE proteins removed (magenta curve: Syx only; blue curve: Protein Free) or if SNAP-25 is truncated to simulate BoNT/E cleavage (green curve: BoNT/E in the absence of V_C peptide; red curve: BoNT/E in the presence of V_C peptide). *b)* Optimization of V_C peptide concentration by measurement of red fluorescence during green excitation from a bulk mixture of 5 nM v-SNARE vesicles labeled with 2% DiD and 10 nM t-SNARE vesicles labeled with 2% DiI. Bulk lipid mixing was enhanced comparably at 2 μM (green curve) and 4 μM V_C peptide (black curve) and much less so at 0.5 μM V_C peptide (purple curve).

Figure 3-3

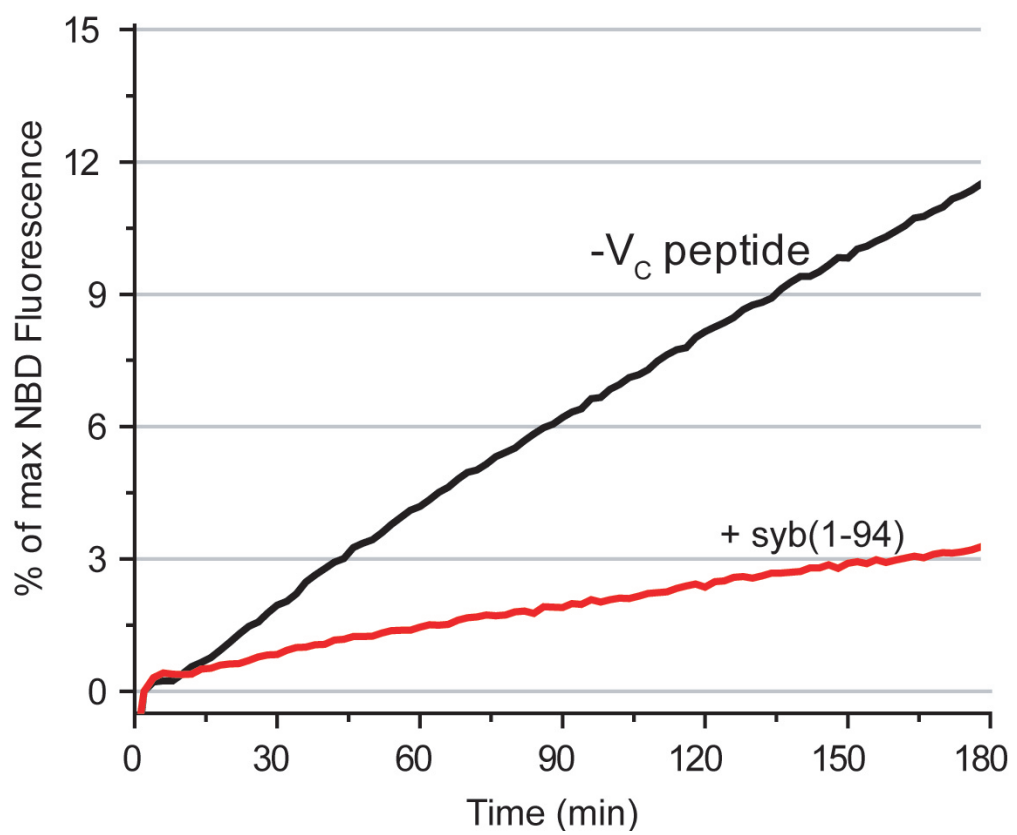
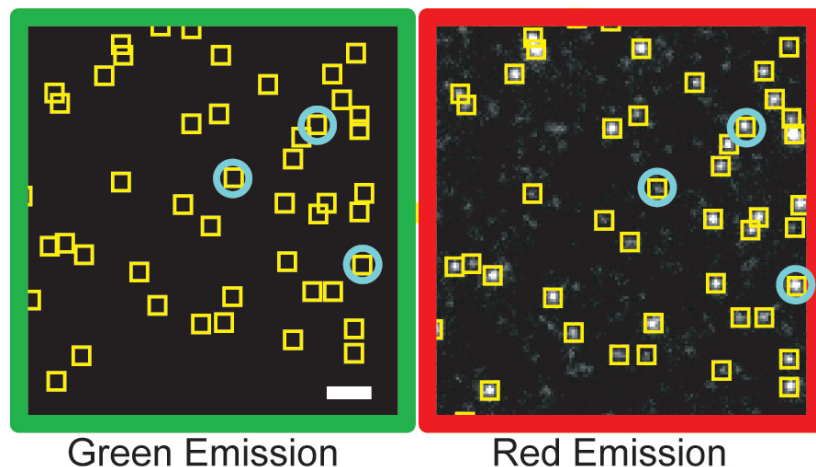


Figure 3-3. Bulk Lipid Mixing Assay from NBD Dequenching

Assay carried out using the dequenching method of Weber *et al.* (Weber et al., 1998). The v-SNARE vesicles were reconstituted with 1.5% NBD-PE and 1.5% Rhodamine-PE and t-SNARE vesicles were unlabeled. The extent of lipid mixing was monitored by NBD fluorescence, which is largely quenched in the absence of fusion due to efficient FRET from NBD to Rhodamine. Vesicles were mixed at a 9:1 t-SNARE vesicle: v-SNARE vesicle ratio with t-SNARE vesicles at 60 nM (black curve). The rate of lipid mixing slows in the presence of 10 μM syb(1-94) (red curve).

Figure 3-4

a. 633 nm excitation



b. 514 nm excitation

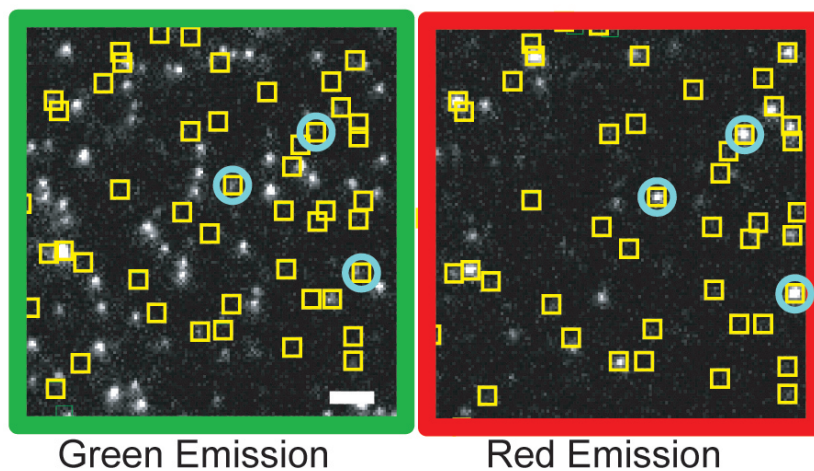


Figure 3-4. Alternating Laser Excitation of Tethered Vesicles with Two-Color Imaging

Example images from the tethered vesicle assay after incubation of tethered v-SNARE vesicles with t-SNARE vesicles for 140 min. *a*) On excitation at 633 nm DiD fluorescence from each tethered v-SNARE vesicle gives rise to puncta in the red emission channel, enabling location of each tethered v-SNARE vesicle. Yellow boxes mark positions of tethered v-SNARE vesicles in both the red and green images. No green emission appears. *b*) Subsequent excitation at 514 nm locates green t-SNARE vesicles (DiI green emission), most of which are non-specifically bound and do not co-localize with the v-SNARE vesicle locations. For those t-SNARE vesicles that co-localize with v-SNARE vesicles, fusion is detected as a greatly enhanced brightening of the red emission on 514 nm excitation. Several examples of docked and fused vesicle pairs are circled. Scale bar = 3.0 μ m.

Figure 3-5

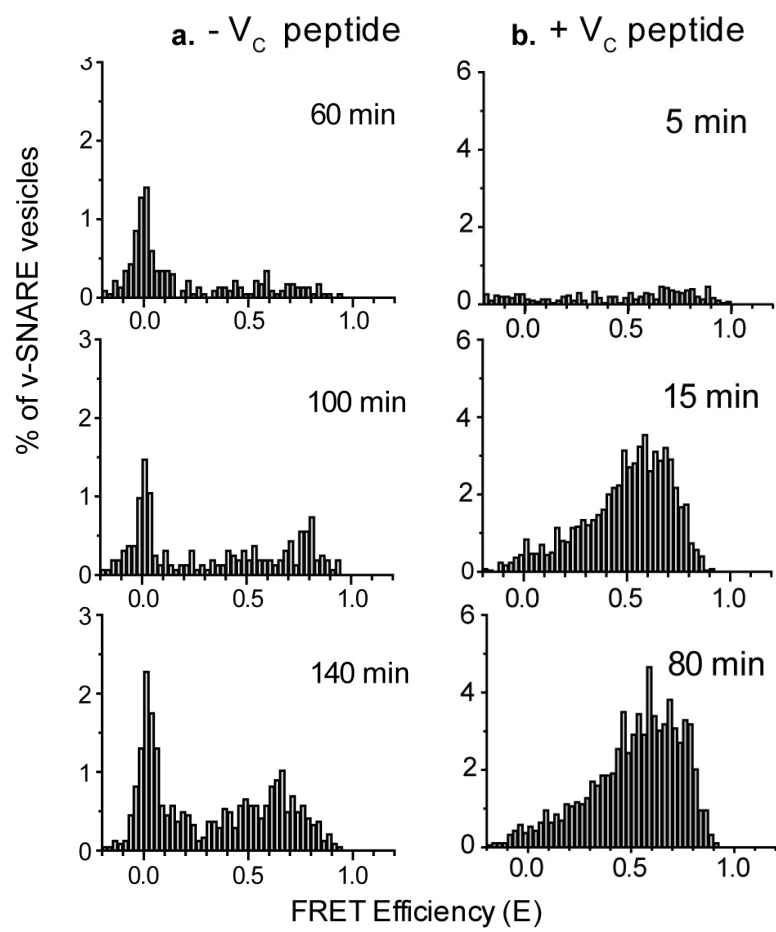


Figure 3-5. FRET Efficiency Histograms vs Reaction Time

Sparsely tethered v-SNARE vesicles were incubated with a 10 nM solution of t-SNARE vesicles *a*) in the absence and *b*) in the presence of 5 μ M V_C peptide. After the specified reaction time, excess (undocked) t-SNARE vesicles were rinsed away. Histograms of DiI to DiD FRET efficiency E (Eq. 1) are presented only for the subset of v-SNARE vesicles that were co-localized with a t-SNARE vesicle. Normalization accounts for variations in the total number of v-SNARE vesicles observed for each sample. Reaction times as shown. The strong peaks at $E = 0$ are due to false co-localization events.

Figure 3-6

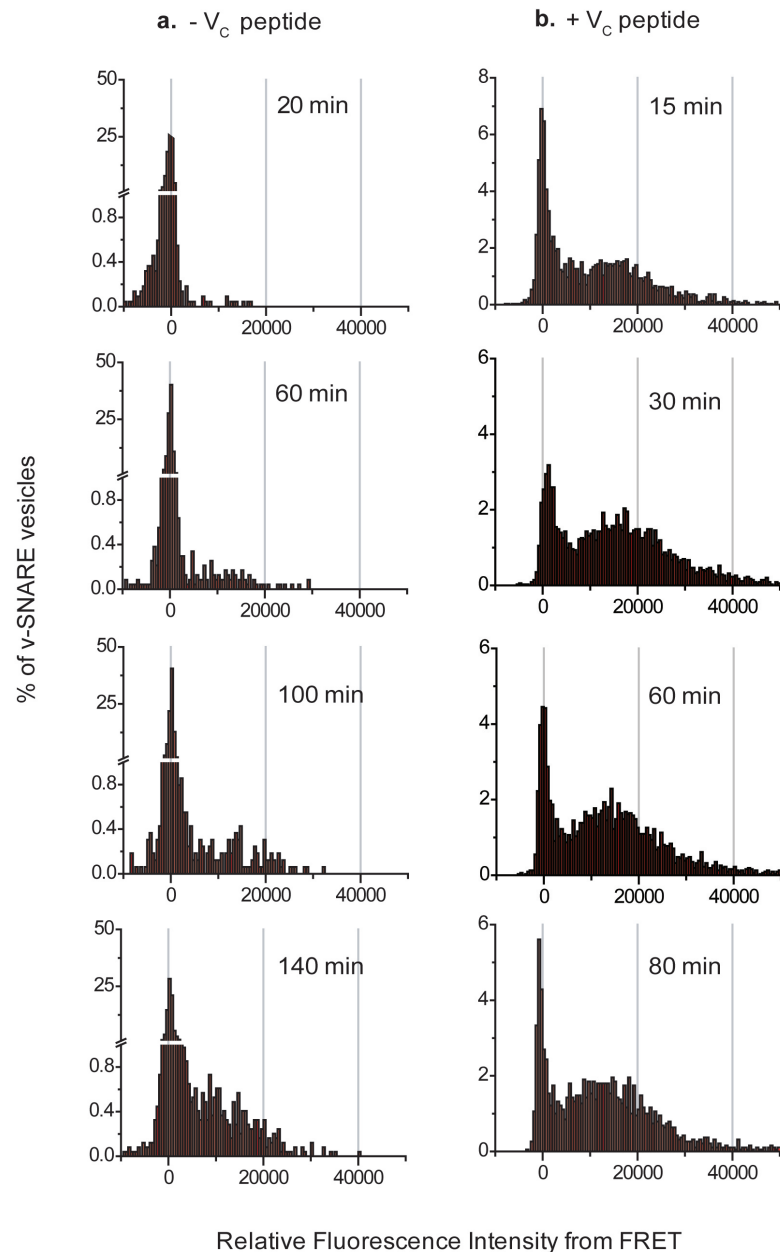


Figure 3-6. Histograms of FRET Intensity for Single, Tethered v-SNARE Vesicles

Tethered DiD-labeled v-SNARE vesicles were incubated with 10 nM Dil-labeled t-SNARE vesicles for: *a*) 20, 60, 100, and 140 min in the absence of V_C peptide and *b*) 15, 30, 60 and 80 min in the presence of 5 μM V_C peptide. At the specified reaction time, excess t-SNARE vesicles were rinsed away and the surface was imaged over several fields of view for up to 5 min using alternating laser excitation. The fluorescence intensity due to FRET from Dil to DiD, I_{FRET}^{514} , was determined for each v-SNARE vesicle after correcting for two sources of cross-talk (Eq. 15). The FRET intensity values are presented in the histograms, which are normalized to account for variations in the number of v-SNARE vesicles imaged at each reaction interval. The large peak centered at zero reflects the population of v-SNARE vesicles that have not docked with a t-SNARE vesicle, that have docked with a t-SNARE vesicle without measurable FRET, or that are experiencing a “false co-localization”. Inclusion of V_C peptide enhances the fraction of v-SNARE vesicles that undergo FRET after a given reaction time.

Figure 3-7

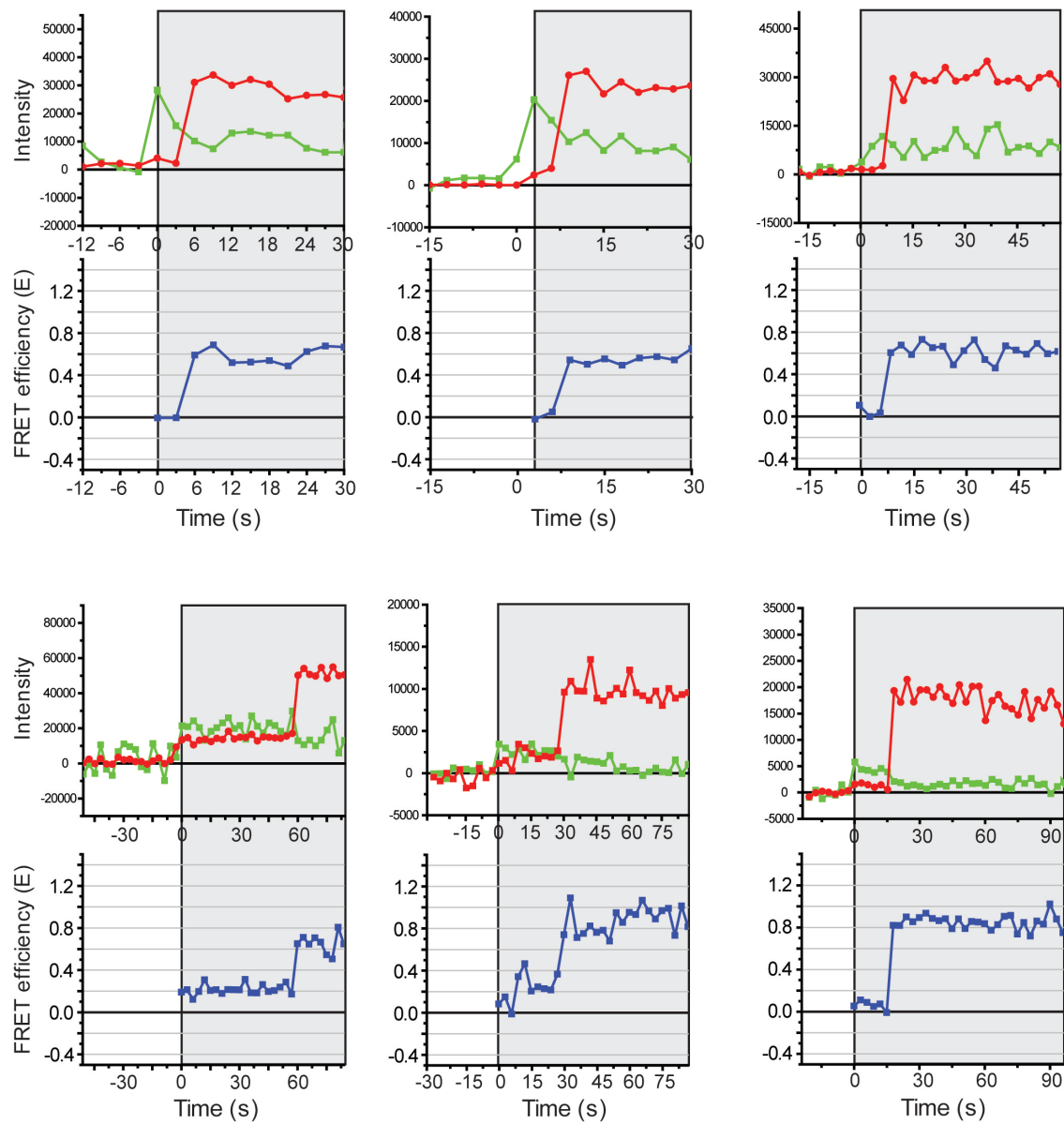


Figure 3-7. Intensity and FRET Efficiency Traces of Individual Docking and Fusion Events.

Background-subtracted, integrated green and red intensities during 514 nm excitation for six well-isolated docking and fusion events observed with 3-s time resolution. Visual inspection of the movie determined the time during which the vesicles were stably co-localized (indicated by gray shading). The corresponding absolute FRET efficiency E (Eq. S2) of the vesicle pair is plotted in blue below the intensity traces. When the vesicles first co-localize the FRET efficiency is low, $E = 0 - 0.25$. The pair then makes an abrupt transition to a high FRET state, $E = 0.5 - 0.95$. For several fusion events, we did not observe a low-FRET state. We interpret these as fast fusion events with $\tau_{\text{fus}} < 3$ s.

Figure 3-8

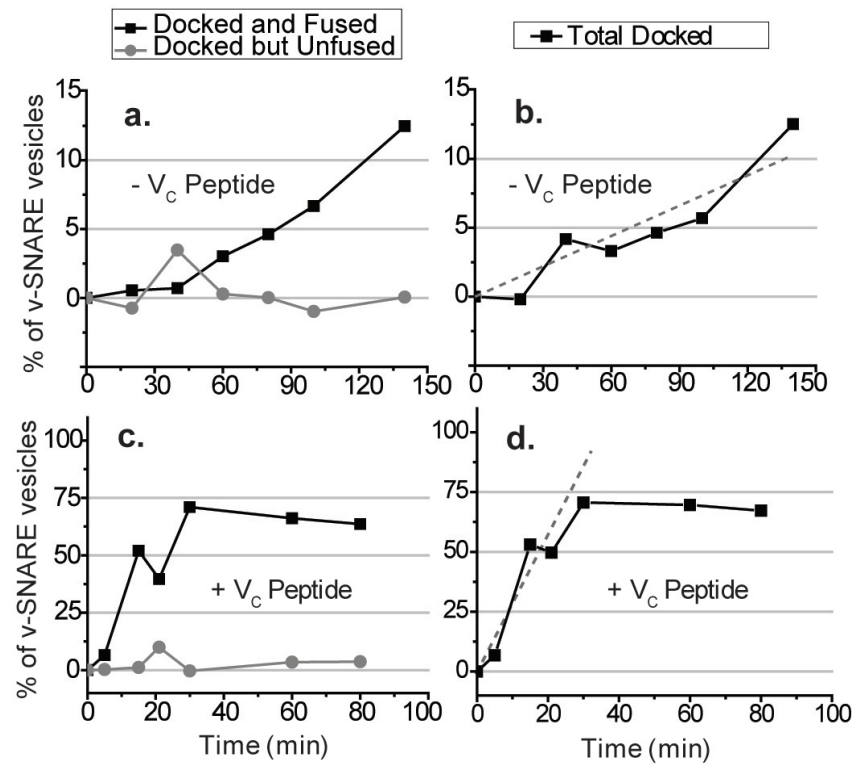


Figure 3-8. Docking and Fusion vs Time in Tethered-Vesicle Assay

Percentage of tethered v-SNARE vesicles that had docked but not fused with a t-SNARE vesicle (grey data points) or docked and fused with a t-SNARE vesicle (black data points) at each reaction time, as determined absolute FRET efficiency. The t-SNARE vesicle concentration was 10 nM. *a*) Without V_C peptide. *c*) In the presence of 5 μ M V_C peptide. Docked but unfused curves are corrected for false co-localizations between a tethered v-SNARE vesicle and a t-SNARE vesicle; see Experimental Procedures. The total docking curves in panels *b* and *d* are the sum of the docked but unfused and docked and fused curves in panels *a* and *c*. Docked but unfused curves are corrected for false co-localizations between a v-SNARE vesicle and a t-SNARE vesicle. The dotted lines represent the linear fits used to determine $k_{dock,teth}$.

Figure 3-9

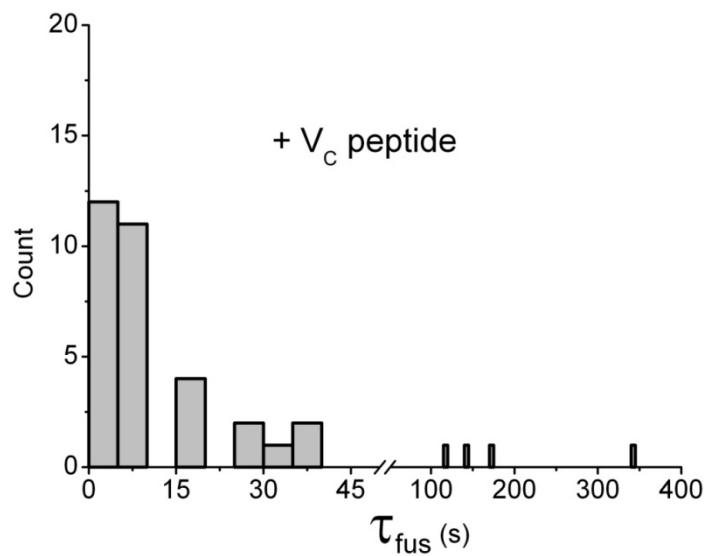


Figure 3-9. Histogram of τ_{fus} for SingleVesicle Fusion Events with V_C Peptide

Histogram showing the dwell time in the docked but unfused state for 36 fusion events observed in real time using the tethered vesicle assay in the presence of V_C peptide at 5 μM . Data obtained with 3 s time resolution. See Fig. S9 for six examples of real-time FRET traces. Fig. 3-14 shows an example of a single fusion event.

Figure 3-10

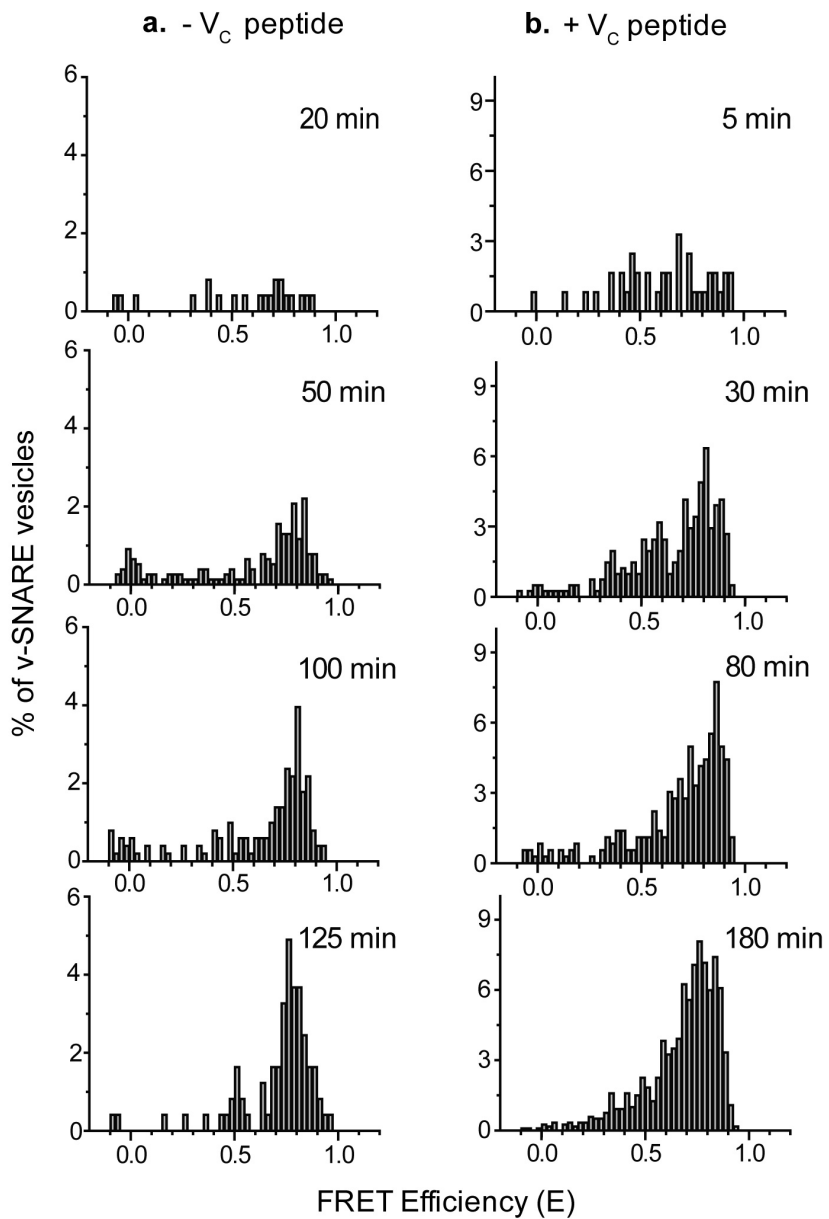


Figure 3-10. FRET Efficiency Histograms for Bulk Fusion Assay vs Reaction Time

10 nM t-SNARE vesicles labeled with 2% DiI were mixed with 5 nM v-SNARE vesicles labeled with 2% DiD *a*) without V_C peptide or *b*) in the presence of 5 μM V_C peptide. At the specified reaction times, the vesicle mixture was sampled, diluted, and plated onto glass for FRET analysis of co-localized v-SNARE/t-SNARE vesicle pairs. FRET efficiency histograms are normalized to account for variations in the total number of v-SNARE vesicles examined at each time point.

Figure 3-11

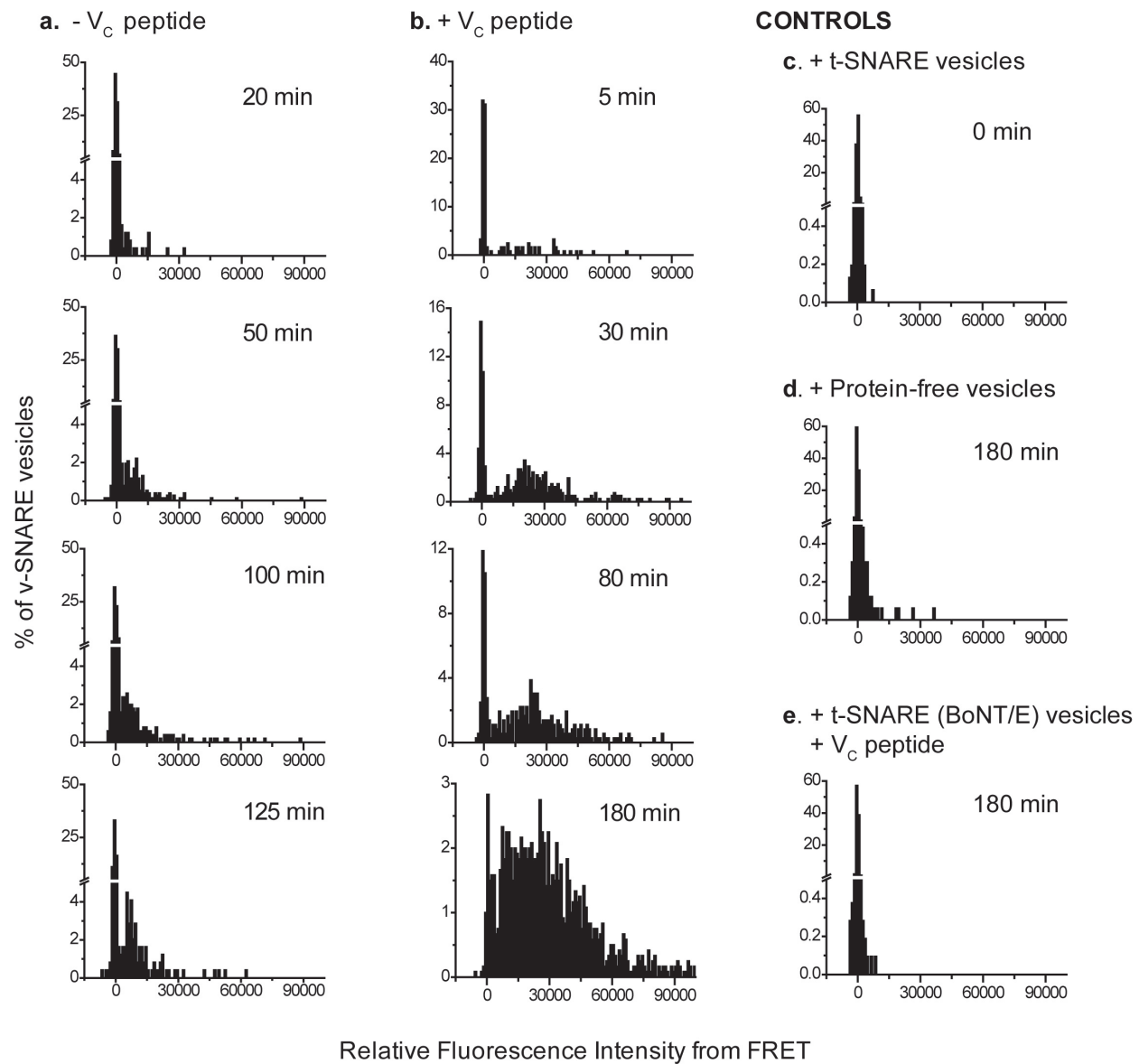


Figure 3-11. Histograms of FRET Intensity for Single v-SNARE Vesicles from Bulk Fusion Assay

5 nM v-SNARE vesicles labeled with 2% DiD were mixed with 10 nM t-SNARE vesicles labeled with 2% DiI *a)* without V_C peptide or *b)* in the presence of 5 μM V_C peptide. At the specified reaction time, the vesicle mixture was sampled, immobilized on glass, and imaged over several fields of view for up to 10 min. Fluorescence intensity due to FRET from DiI to DiD, I_{FRET}^{514} , was determined for each v-SNARE vesicle after correcting for two sources of cross-talk (Eq. 15). The histograms are normalized to account for variations in the number of v-SNARE vesicles imaged at each reaction interval. In each histogram the peak centered at zero reflects the population of v-SNARE vesicles that have not yet docked with a t-SNARE vesicle, that have docked with a t-SNARE vesicle without measurable FRET, or that are experiencing a false co-localization. Inclusion of V_C peptide greatly enhances the fraction of v-SNARE vesicles that undergo FRET after a given reaction time. *Controls:* *c)* v-SNARE vesicles were immobilized sparsely onto a glass coverslip. The coverslip was thoroughly rinsed and then t-SNARE vesicles were immobilized sparsely onto the same glass coverslip. *d)* 5 nM v-SNARE vesicles were mixed with 10 nM protein free vesicles labeled with 2% DiI for 180 min, sampled, and immobilized on glass. *e)* 5 nM v-SNARE vesicles were mixed with 5 μM V_C peptide and 10 nM 2% DiI-labeled t-SNARE vesicles designed to mimic BoNT/E cleavage for 180 min, sampled, and immobilized on glass.

Figure 3-12

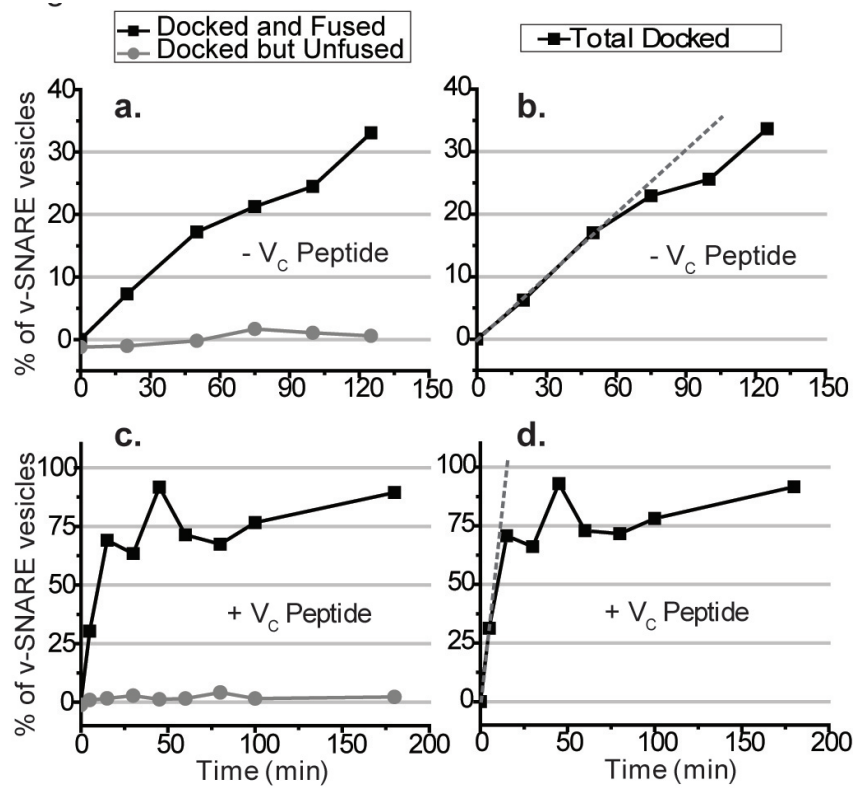


Figure 3-12. Docking and Fusion vs Time in Bulk Assay

The percentage of free v-SNARE vesicles that had docked but not fused with a free t-SNARE vesicle (grey data points) or docked and fused with a free t-SNARE vesicle (black data points) at each reaction time is shown, as determined by a vesicle pair's absolute FRET efficiency. Mixtures were 10 nM t-SNARE vesicles and 5 nM v-SNARE vesicles without V_C peptide (*a* and *b*) and in the presence of 5 μ M V_C peptide (*c* and *d*). The total docking curves in panels *b* and *d* are the sum of the docked and fused and the docked but unfused curves in panels *a* and *c*. Docked but unfused curves are corrected for false co-localizations between a v-SNARE vesicle and a t-SNARE vesicle. The dotted lines represent the linear fits to the total docking curves that used to determine $k_{dock,bulk}$.

Figure 3-13

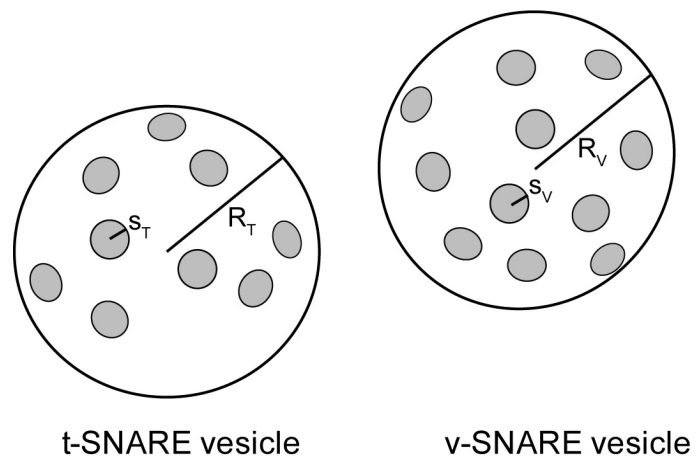


Figure 3-13. Collision Encounter Model

The v-SNARE and t-SNARE vesicles are modeled as spheres of equal size. The SNARE proteins were modeled as absorbing disks that occupy a fraction of the surface area. The absorbing disks on both v-SNARE and t-SNARE vesicles have a radius of 2 nm. There are 45 disks on the v-SNARE vesicle and 65 disks on the t-SNARE vesicle.

Figure 3-14

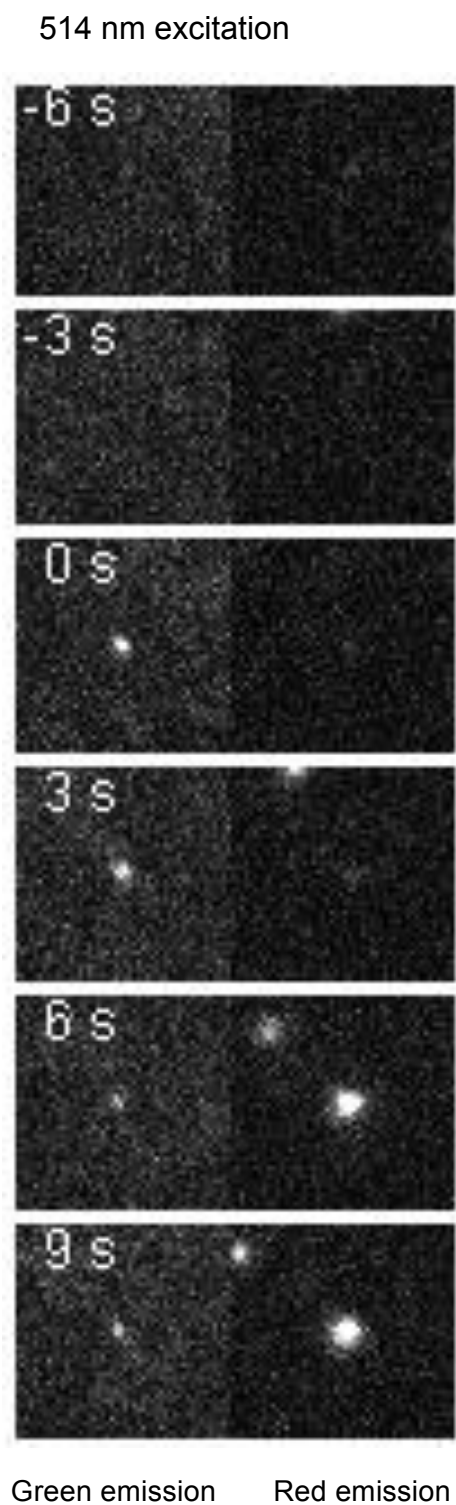


Figure 3-14. Montage of A Single Docking and Fusion Event with 3 s Time

Resolution

The left half of the montage shows fluorescence detected in the green channel and the right half of the montage shows fluorescence detected in the red channel at the same position in space during excitation at 514 nm. At $t = 0$, a green fluorescent, DiI-labeled t-SNARE vesicle adsorbs from solution and co-localizes with a tethered v-SNARE vesicle. The position of the tethered v-SNARE vesicle labeled by red-fluorescent DiD was confirmed using 633 nm excitation (not shown). The t-SNARE vesicle remains co-localized without significant FRET (docked but unfused) with the v-SNARE vesicle for two frames. By the third frame the green fluorescence has disappeared simultaneous with the appearance of fluorescence in the red channel due to FRET. The delay between docking and fusion is $\tau_{fus} = 6$ s for this particular event.